Neutral Hexacoordinate Silicon Complexes. Synthesis, Structure, and Stereodynamics: Evidence for Two Nondissociative Ligand-Exchange Mechanisms[1]

Daniel Kost,*,† Inna Kalikhman,*,† and Morton Raban‡

Contribution from the Departments of Chemistry, Ben Gurion University of the Negev, Beer Sheva 84105, Israel, and Wayne State University, Detroit, Michigan 48202

Received June 22, 1995[⊗]

Abstract: Novel hexacoordinate silicon compounds **1**−**4** with two identical bidentate ligands, respectively, are readily prepared in high yields from the reaction of $XSiCl_3$ (X = H, Me, Ph, Cl) with the *O*-trimethylsilyl derivatives of *N,N*-dimethyl carbohydrazides **6**. The NMR spectra of all compounds indicate that a single diastereomer is present in solution, of the possible six, within NMR detection limits. The published X-ray crystallographic structure of one of the complexes, as well as an analysis of the ^1H, ^{13}C, and ^{29}Si NMR spectra and their temperature dependence, conforms to an octahedral geometry with the oxygen ligands and the pair of monodentate ligands *cis* to each other, respectively, and the nitrogens in a *trans* position. All of the complexes show temperature dependence of their NMR spectra, characteristic of fluxional behavior. Two rate processes (topomerizations) take place on the NMR time scale in compounds **1**−**3**, at activation free energies ranging, respectively, between 10.6 and 16.4 kcal/mol, and 15.0 and 18.5 kcal/mol. A single process is observed for the C_{2v} symmetric **4** complexes. A remarkable solvent dependence of barriers is observed, suggesting that ligand site exchange is associated with dissociation or weakening of Si−ligand bonds. The simultaneous exchange of *N*-methyl groups and benzyl methylene protons in **3d** is evidence that no Si−N bond cleavage and chelate ring opening take place during topomerization. The persistence of ^{29}Si−^{19}F one-bond coupling, observed in the ^{29}Si NMR spectrum at temperatures well above the fast exchange limit temperature, proves that no ionic dissociation of the Si−halogen bond takes place. It is concluded that topomerization occurs in a nondissociative, intramolecular ligand site exchange process. A likely mechanism that accounts for all of these observations is a 1,2-shift of adjacent ligands, X and Cl, or the two oxygen ligands, *via* a "bicapped tetrahedron" intermediate or transition state.

1. Introduction

Hypervalent silicon compounds have received considerable attention and have been extensively reviewed.[2] A fundamental characteristic of hypervalent silicon complexes is their ease of inter- and intramolecular ligand site exchange.[2] As early as 1968 Mueterties and co-workers reported on site exchange reactivity of pentavalent polyfluorosilicates.[3] The mechanism of exchange, whether strictly intramolecular or catalyzed by impurities, was later disputed by Janzen and co-workers,[4] but was finally confirmed to be both intermolecular and purely intramolecular.[5] The question of exchange mechanism in silicon complexes continued to be of interest as more hexacoordinate compounds were prepared and reported.[2d] Like pentacoordinate silicon complexes,[6] they show diverse interconversion and exchange reactivity. Thus, both inter-[7] and intramolecular[8] ligand exchange reactions were reported in hexacoordinate complexes. Recently Corriu and co-workers reported an intramolecular dissociative process in hexacoordinate chelates, in which two identical dimethylamino coordination sites competitively coordinate to silicon in a dynamic process observed by NMR.[9] Presumably this exchange of dimethylamino coordination takes place *via* a heptacoordinate intermediate (or transition state) in which both ligands are simultaneously loosely bound. It is evident that many different exchange mechanisms may operate in this type of compound, and the exact pathways are far from being fully understood.

This paper describes the synthesis, structure, and stereodynamic behavior of novel neutral hexacoordinate silicon complexes **1**−**4**, in which a series of new bidentate ligands, based on 1,1-dimethyl-2-acylhydrazine $Me_2NNHCOR$ (**5**, R = Me, Ph, CF_3, CH_2Ph), have been incorporated. The preparation of pentacoordinate silicon chelates with **6**, the O-trimethylsilylated derivative of **5**, has been described previously.[10] Due to the flexibility of this family of ligands, and the presence of the geminal *N*-methyl groups, a detailed study of the stereodynamics of the compounds is possible.[11] An analysis of ligand-site exchange is presented, and new mechanistic pathways are proposed on the basis of these observations.

2. Synthesis and Structure

Complexes **1**−**4** were readily prepared by the reaction of O-trimethylsilylated *N,N*-dimethyl hydrazides of carboxylic

† Ben Gurion University of the Negev.

‡ Wayne State University.

⊗ Abstract published in *Advance ACS Abstracts*, November 1, 1995.

(1) For a preliminary communication see: Kalikhman, I.; Kost, D.; Raban, M. *J. Chem. Soc., Chem. Commun.* **1995**, 1253.

(2) For recent reviews see: (a) Tandura, St. N.; Alekseev, N. V.; Voronkov, M. G. *Top. Curr. Chem.* **1986**, *131*, 99. (b) Corriu, R. J. P.; Young, J. C. Hypervalent Silicon Compounds. In *The Chemistry of Organic Silicon Compounds*; Patai, S., Rappoport, Z., Eds.; Wiley: Chichester, England, 1989; p 1241. (c) Corriu, R. J. P. *J. Organomet. Chem.* **1990**, *400*, 81. (d) Chuit, C.; Corriu, R. J. P.; Reye, C.; Young, J. C. *Chem. Rev.* **1993**, *93*, 1371. (e) Wong, C. Y.; Woollins, J. D. *Coord. Chem. Rev.* **1994**, *130*, 175.

(3) Klanberg, F.; Muetterties, E. L. *Inorg. Chem.* **1968**, *7*, 155.

(4) Marat, R. K.; Jansen, A. F. *Can. J. Chem.* **1977**, *55*, 1167; 3845.

(5) Damrauer, R.; Danahey, S. E. *Organometallics* **1986**, *5*, 1490.

(6) Carré, F.; Corriu, R. J. P.; Kpoton, A.; Poirier, M.; Royo, G.; Young, J. C. *J. Organomet. Chem.* **1994**, *470*, 43 and references therein.

(7) Farnham, W. B.; Whitney, J. F. *J. Am. Chem. Soc.* **1984**, *106*, 3992.

(8) (a) Breliere, C.; Corriu, R. J. P.; Royo, G.; Zwecker, J. *Organometallics* **1989**, *8*, 1834. (b) Breliere, C.; Carré, F.; Corriu, R. J. P.; Douglas, W. E.; Poirier, M.; Royo, G.; Wong Chi Man, M. *Organometallics* **1992**, *11*, 1586.

(9) Carré, F.; Chuit, C.; Corriu, R. J. P.; Fanta, A.; Mehdi, A.; Reye, C. *Organometallics* **1995**, *14*, 194.

0002-7863/95/1517-11512$09.00/0

acids (**6**) with polychlorosilanes $XSiCl_3$ (**7**, X = H; **8**, X = Me; **9**, X = Ph; **10**, X = Cl), at ambient temperature, in essentially quantitative yields (eq 1). The reactions were complete within a few minutes, during which the temperature rose spontaneously. This is a particularly convenient route to hexacoordinate chelates, since the excess polychlorosilane and the byproduct **11** are volatile and easily removed.

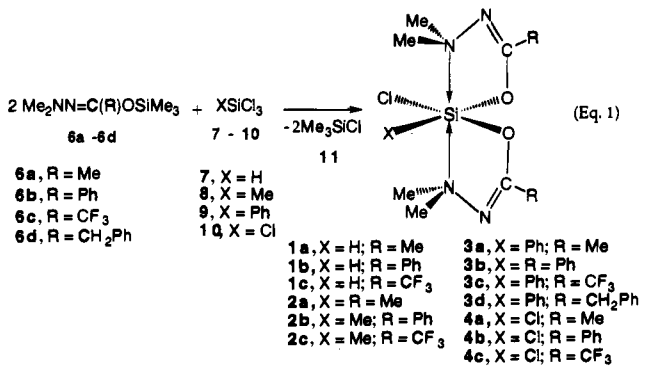

The assignment of structures **1**–**4** to the complexes formed in this reaction requires the demonstration of three structural features: (a) the incorporation of two ligands in the complex, (b) the bidentate nature of both ligands and the geometry of the complex, and (c) the configuration of the octahedral complex. For one of these compounds, **2b**, these features were recently confirmed in the solid state by an X-ray crystallographic study.[11b] The solution structure of this and other members of the series needs further discussion.

The stoichiometry of these compounds was easily demonstrated by elemental or mass spectrometry, as well as from relative integrated signal intensities of the R and X groups in the ^1H NMR spectra; both the analysis and the NMR spectra clearly showed a 2:1 ratio of the bidentate ligand relative to silicon.

Demonstration of 2:1 stoichiometry alone is not sufficient for the assignment of hexacoordinate structure. It is conceivable that the presumably bidentate ligands could also be monodentate, with oxygens forming covalent bonds to silicon, and the dimethylamino groups either coordinated to silicon or not. Thus, tetravalent compounds with the 2:1 R:X ratio are possible. Alternatively we can also conceive of a bicapped tetrahedral geometry with longer dative bonds between the dimethylamino groups and the silicon atom, intermediate between those in tetracoordinate and octahedral hexacoordinate geometries. Such bicapped tetrahedral structures have been reported recently for hexacoordinate silicon chelates in the solid state.[12]

Evidence for the bidentate nature of the ligands in these complexes and for the octahedral geometry was obtained from ^{29}Si chemical shifts and $^{29}Si-H$ coupling constants. It has been shown previously that a change from tetra- to hexacoordinate silicon is associated with a 70–80 ppm upfield shift, provided the remaining environment is kept unchanged.[13] Table 1 lists the ^{29}Si chemical shifts for **1**–**4**. These shifts may be compared with the analogous tetracoordinate compounds $HClSi(O^-)_2$ (**12**, a polychlorosiloxane, δ = −64.8 ppm, analogous to **1**, δ = −136.5 to −137.7 ppm)[14] and $MeClSi(OSiMe_3)_2$ (**13**, δ = −46.2 ppm, analogous to **2**, δ = −121.0 to −124.5 ppm).[14] Indeed the comparison of ^{29}Si chemical shifts reveals substantial upfield changes, $\Delta\delta$ = 71.7–72.9 ppm for **1** and 74.8–78.3 ppm for **2**, precisely as expected for hexacoordinate complexes. By contrast, a remarkable *lack* of trend in $\delta(^{29}Si)$ was observed in a series of neutral complexes, reported as "formally hexacoordinate", the bicapped tetrahedral complexes.[2d,8a,12] In this series a change from the tetracoordinate silane precursor to pentacoordination was associated by a *ca.* 4 ppm upfield shift, and a further change to hexacoordination resulted in no significant change in $\delta(^{29}Si)$. We may thus conclude from the trend in $\delta(^{29}Si)$ in the present study not only that the coordination number to silicon is 6, but also that the geometry is indeed octahedral.

Table 1. ^{29}Si Chemical Shifts and $^{29}Si-^1H$ Coupling Constants for Compounds **1**–**4**

compd	$\delta(^{29}Si)$, ppm	$^1J(Si-H)$, Hz	compd	$\delta(^{29}Si)$, ppm
1a	−137.7	341.8	**3a**	−128.8
1b	−137.2	340.2	**3b**	−131.8
1c	−136.5	344.4	**3c**	−132.7
2a	−121.0		**3d**	−132.6
2b	−121.7		**4a**	−147.2
2c	−124.5		**4b**	−145.9
			4c	−146.2

Additional evidence for hexacoordination is based on $^{29}Si-^1H$ coupling constants (Table 1). The analogy is taken from SiF compounds: increasing the coordination number of silicon while keeping the same number of electronegative (fluorine) ligands attached to it resulted in a decrease in the $^{29}Si-^{19}F$ coupling constant.[2a,8,15] In analogy one might expect the Si–H coupling constant to decrease with increasing coordination number. Thus, $^1J(^{29}Si-^1H)$ = 381 Hz has been reported for **12**,[14] *ca.* 40 Hz greater than the values reported for compounds **1** in Table 1, indicating that the latter are hexacoordinate. A similar trend for the change in coordination number from 4 to 5 was recently reported:[16,17] an increase of the coordination in anionic silicates was accompanied by a decrease in $^1J(^{29}Si-^1H)$ of *ca.* 65 Hz, in accord with the changes reported in this work. It follows from this discussion that the one-bond coupling constant ($^{29}Si-^{19}F$ or $^{29}Si-^1H$) is a sensitive measure of the extent of s-character in the Si–F or Si–H bond.[2a,16,17] For hexacoordinate silicon compounds having a bicapped tetrahedral geometry, however, an *opposite* trend in $^{29}Si-^1H$ coupling constants has been reported.[8a] This may be rationalized as follows: the decrease in s-character which normally accompanies an increase in coordination number and rehybridization at silicon results in a *decrease* in one-bond coupling. However, the change in coordination number in the bicapped tetrahedral complexes is essentially *not associated with rehybridization.* On the contrary, coordination of donor ligands to

(10) (a) Kalikhman, I. D.; Bannikova, O. B.; Petukhov, L. P.; Pestunovich, V. A.; Voronkov, M. G. *Dokl. Akad. Nauk SSSR* **1986**, *287*, 870. (b) Kalikhman, I. D.; Pestunovich, V. A.; Gostevskii, B. A.; Bannikova, O. B.; Voronkov, M. G. *J. Organomet. Chem.* **1988**, *338*, 169. (c) Macharashvili, A. A.; Shklover, V. E.; Struchkov, Yu. T.; Voronkov, M. G.; Gostevskii, B. A.; Kalikhman, I. D.; Bannikova, O. B.; Pestunovich, V. A. *J. Organomet. Chem.* **1988**, *340*, 23. (d) Macharashvili, A. A.; Shklover, V. E.; Struchkov, Yu. T.; Gostevskii, B. A.; Kalikhman, I. D.; Bannikova, O. B.; Voronkov, M. G.; Pestunovich, V. A. *J. Organomet. Chem.* **1988**, *356*, 23.

(11) For preliminary communications see: (a) Kalikhman, I. D.; Gostevskii, B. A.; Bannikova, O. B.; Voronkov, M. G.; Pestunovich, V. A. *Metalloorg. Khim.* **1989**, *2*, 937; *Chem. Abstr.* **1990**, *112*, 1188926r. (b) Mozzhukhin, A. O.; Antipin, M. Yu.; Struchkov, Yu. T.; Gostevskii, B. A.; Kalikhman, I. D.; Pestunovich, V. A.; Voronkov, M. G. *Metalloorg. Khim.* **1992**, *5*, 658. *Chem. Abstr.* **1992**, *117*, 234095w.

(12) Breliere, C.; Carré, F.; Corriu, R. J. P.; Poirier, M.; Royo, G.; Zwecker, J. *Organometallics* **1989**, *8*, 1831.

(13) (a) Cella, J. A.; Cargioli, J. D.; Williams, E. A. *J. Organomet. Chem.* **1980**, *186*, 13. (b) Marsmann, H. C. *NMR* **1981**, *17*, 65. (c) Williams, E. A. In *The Chemistry of Organic Silicon Compounds*; Patai, S., Rappoport, Z., Eds.; Wiley: Chichester, England, 1989; p 511.

(14) Horn, H. G.; Marsmann, H. C. *Makromol. Chem.* **1972**, *162*, 255.

(15) (a) Gibson, J. A.; Ibbott, D. G.; Janzen, A. F. *Can. J. Chem.* **1973**, *51*, 3203. (b) Albanov, A. I.; Gubanova, L. I.; Larin, M. F.; Pestunovich, V. A.; Voronkov, M. G. *J. Organomet. Chem.* **1983**, *244*, 5.

(16) Becker, B.; Corriu, R. J. P.; Guerin, C.; Henner, B.; Wang, Q. *J. Organomet. Chem.* **1989**, *368*, C25.

(17) Bassindale, A. R.; Jiang, J. *J. Organomet. Chem.* **1993**, *446*, C3.

Table 2. Temperature Dependence of ^{1}H NMR Chemical Shifts for **1**−**4** in Toluene-d_8 Solution

compd	X	R	temp, K	δ(N−*Me*), ppm				δ(C−*Me*), ppm		δ(*ortho* H),[a] ppm		
1a	H	Me	280	3.00	2.89	2.65	2.55	1.66	1.65			
			298		2.75			1.67				
1b	H	Ph	300	3.15	2.97	2.73	2.71					
			350		2.93							
1c	H	CF_3	298	2.65	2.51	2.36	2.34					
			345		2.55							
2a	Me	Me	250	2.89	2.84	2.73	2.64	1.63	1.58			
			298		2.75			1.61				
2b	Me	Ph	260	3.09	2.90	2.84	2.71					
			298		2.92							
2c	Me	CF_3	263	2.54	2.35	2.19	2.14					
			298		2.40							
3a	Ph	Me	243	3.02	2.42	2.40	2.12	1.73	1.71	8.80		7.71
			340		2.50			1.75			8.25	
3b	Ph	Ph	253	3.26	2.62	2.57	2.31			8.92		7.75
			340		2.75						8.35	
3c	Ph	CF_3	263	2.85	2.25	2.25	1.88			8.60		7.60
			320		2.20						8.00	
3d	Ph	$PhCH_2$	278	2.99	2.54	2.30	2.14	3.30[b]	3.33[b]	8.82		7.71
								3.06	3.30			
			350		2.20			3.18			8.10	
4a[c]	Cl	Me	298		3.15	2.98		1.87				
			360		3.08			1.87				
4b[c]	Cl	Ph	298		3.27	3.10						
			375		3.19							
4c[c]	Cl	CF_3	298		3.33	3.26						
			398		3.30							

[a] Coalescence of *ortho* protons of the Si−Ph group. All signals are doublets, $J = 8.8$ Hz. [b] Entries represent chemical shifts of each CH_2 proton, four for two AB quartets; J(A−B) = 14 Hz. [c] Spectra were measured on a 90 MHz (JEOL FX-90Q) spectrometer, in nitrobenzene-d_5 solution.

the essentially unchanged tetrahedral silicon in these complexes increases the electron density near the Si−H bond, resulting in an *increase* in one-bond coupling.

In this type of octahedral complex with two monodentate ligands, there are in principle six different diastereoisomers possible (Figure 1): two of them (**I** and **II**) have the pair of monodentate ligands *trans* to each other, and in the other four the arrangement is *cis*. The number of *N*-methyl signals is indicative of the configuration. The symmetry point group for each structure and the expected number of *N*-methyl signals are shown in Figure 1.

The NMR spectra for all of the complexes show that only one isomer predominates in solution, with no detectable amounts of other diastereomers. The spectra are temperature dependent in various solvents, as will be discussed in the following sections. However, at the slow exchange limit temperatures relative to the NMR time scale, all complexes with different monodentate ligands (**1a**−**c**, **2a**−**c**, **3a**−**d**) display four different signals in their ^{1}H and ^{13}C NMR spectra, for the four *N*-methyl groups (Tables 2 and 3). This is consistent only with the *cis* arrangement of ligands, as depicted in Figure 1 (structures **III**−**VI**). This result is further supported by the observation that the two chelate cycles are diastereotopic: the R groups as well as the imidic carbons on both rings are nonequivalent, as expected for structures **III**−**VI**. For compounds **4a**−**c**, in which both ligands are chlorine atoms, the slow exchange spectra show only two *N*-methyl signals, as expected for structures **IV** and **VI** in Figure 1. The structural possibilities have thus been further narrowed down to only these two geometries.

There may, in principle, be three reasons for the appearance of NMR signals due to only one diastereomer in solution: (i) rapid interconversion between isomers relative to the NMR time scale, (ii) substantially lower free energy of one of the isomers, leading to its predominance in solution within the NMR detection limit, and (iii) accidental equivalence of signals from different stereoisomers. The third possibility may be ruled out immediately: while accidental equivalence may be quite common for one or two different signals in different isomers, the likelihood that *all* of the NMR active groups in the ^{1}H, ^{13}C, and ^{29}Si NMR spectra are equivalent and isochronous for *all* of the possible diastereomers is definitely negligible.

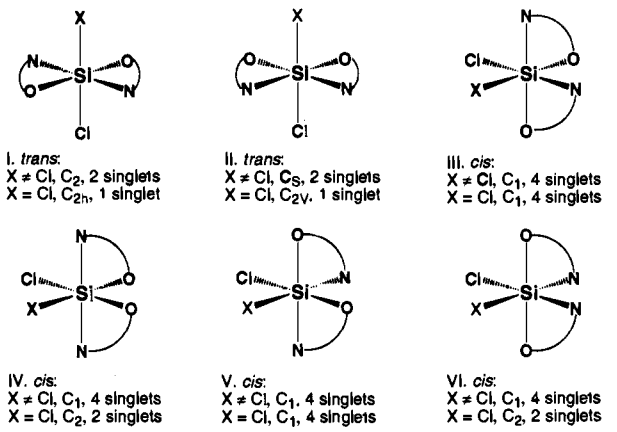

Figure 1. Schematic presentation of six possible diastereoisomeric geometries. The symmetry point group and expected number of *N*-methyl signals in the NMR (at the slow exchange limit) in the mono- and dichloro complexes are given under each structure.

Possibility i, that rapid interconversion of stereoisomers leads to the observation of averaged signals only, may be excluded for the following reasons: the exchange of ligand sites leading to either topomerization or diastereomerization is likely to proceed through similar mechanisms (direct exchange of adjacent ligands, intermolecular exchange, pseudorotation, or similar ligand-rearrangement processes). It follows that the barriers for these exchanges should be similar or at least within similar free energy ranges. Therefore, lowering the temperatures below the slow exchange limit for topomerization should also bring about slow interconversion of diastereomers. While slow exchange of topomers results in decoalescence of signals due to diastereotopic groups, slow exchange of diastereomers should result in decoalescence of *all* of the signals. However, in none

Table 3. Temperature Dependence of ^{13}C NMR Chemical Shifts for **1–4** in Toluene-d_8 Solution[a]

compd	X	R	temp, K	δ(N–*Me*), ppm				δ(*C*=N), ppm		δ(*ortho C*), ppm	
1a	H	Me	298	50.8	50.5	49.8	49.0	166.9	166.7		
			330		50.4			166.8			
1b	H	Ph	298[b]	51.1	51.1	50.3	49.6	164.7	164.5		
1c	H	CF_3	298[b]	50.7	50.2	49.3	48.8	157.3[c]	157.0[c]		
2a	Me	Me	263	51.8	51.0	50.7	49.6	166.0	165.5		
			298		51.2			165.7			
2b	Me	Ph	263	52.6	51.6	51.2	50.4	164.0	163.8		
			298		51.4			163.9			
2c	Me	CF_3	263	51.3	50.4	50.3	49.3	156.3[c]	156.1[c]		
			298		50.7			156.2[c]			
3a	Ph	Me	298	52.0	52.0	50.8	50.4	165.7	165.6	139.3	136.0
			330		51.4			165.7		137.4	
3b	Ph	Ph	298	52.7	52.5	51.4	50.9	165.0	163.9	139.3	136.2
			330		52.1			164.5		137.5	
3c	Ph	CF_3	270	51.6	51.6	50.5	50.2	156.9[c]	156.2[c]	138.9	135.8
			298		50.8			156.7[c]		137.4	
3d[d]	Ph	$PhCH_2$	270	51.8	51.8	50.9	50.2	166.7	166.6	138.9	136.0
			330		50.9			166.6		138.7	
4a[e]	Cl	Me	298[b,f]	52.0		51.2		165.6			
4b[e]	Cl	Ph	298[b,f]	52.9		52.2		163.0			
4c[e]	Cl	CF_3	298[b,f]	52.1		51.8		156.1[c]			

[a] Only the well-resolved signal pairs are included in the table. [b] ^{13}C coalescence above 380 K. [c] Quartet centered at given δ. $^2J(^{19}F-^{13}C)$ ranges between 36 and 39 Hz. [d] At 270 K two signals were observed for the benzylic carbons at 38.2 and 38.0 ppm; at 330 K these signals had coalesced to one, at 38.1 ppm. [e] Nitrobenzene-d_5 solution. [f] At the slow exchange limit two N–*Me* signals are observed; see the text.

of the complexes studied was such signal splitting observed: the X groups in **1–4**, as well as silicon in the ^{29}Si NMR spectra, always showed single resonances. We may therefore conclude that the rate processes observed correspond to topomerizations and not to diastereomerizations. Furthermore, the equilibrium constant between diastereomers is expected to differ from one: if splitting of the *N*-methyl signals at low temperatures were due to freezing out of such equilibrium, one should expect to observe *unequal* signal intensities due to different isomers. The fact that in all cases the decoalesced signal intensities were equal, within measurable limits, strongly indicates that the exchange is between equally populated species, i.e., identical or enantiomeric complexes, and hence corresponds to topomerization.

We are thus left with option ii, that interconversion of diastereomers is not observed because of unfavorable equilibrium constants, which strongly favor a single, more stable, diastereomer in solution.

Direct structural evidence for one of the complexes (**2b**) has previously been obtained through X-ray crystallographic analysis.[11b] The structure obtained clearly demonstrated a nearly octahedral arrangement around silicon, corresponding to geometry **IV** (Figure 1). The two monodentate ligands in **2b** occupy *cis* positions, as has been found for several other hexacoordinate bischelates.[2] Since all of the complexes studied have very similar behavior in solution (a single predominant stereoisomer, analogous NMR spectra, similar rate processes) it may be concluded that the structure found for **2b** represents the predominant isomer observed for all complexes in solution. This suggests, along with the NMR evidence discussed above, that the single configuration of **1–4** observed in solution may be assigned to **IV**.

One other compound (**14**) was previously reported with a similar coordinative environment (i.e., the same ligand atoms are connected to silicon).[18] However, the reported X-ray crystal structure indicated that in **14** the nitrogen atoms were in a *cis* configuration and the oxygens were *trans*, corresponding to geometry **VI** (Figure 1), in contrast with the geometry reported for **2b**. This difference is difficult to rationalize, and may result from the reduced flexibility of the bidentate ligands in **14** relative to **1–4**.

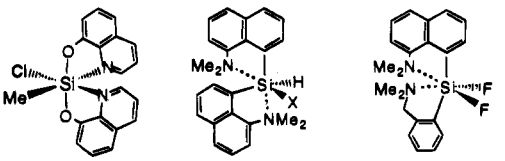

14 **15** X = H, **16** X = F **17**

The octahedral geometries found for **2b** and **14** are associated with relatively short Si–N dative bonds (2.036 and 2.015 Å in **2b**;[11b] 2.014 and 2.016 Å in **14**[18]). This is in contrast with the relatively long Si–N distances reported for the bicapped tetrahedral complexes **15–17** (2.60–2.81 Å).[12]

3. Stereodynamic Analysis

3.a. Dynamic NMR Results. The NMR spectra of all complexes, in various solvents, showed the features of only one diastereomer within the NMR detection level. The NMR analysis of complexes **1a–c**, **2a–c**, and **3a–d** in toluene-d_8 solution showed four singlets of equal intensities corresponding to the four *N*-methyl groups at ambient or lower temperatures, in both ^1H and ^{13}C spectra (Tables 2 and 3). In addition, the two R groups on the chelate cycles were nonequivalent, as were the imidic carbons in each of the rings. This is evidence that in all the complexes the two chelate rings are diastereotopic, as are the methyl groups on each nitrogen within each chelate ring. Likewise, the *ortho* phenyl protons and carbons in **3a–d**, in which phenyl is attached to silicon, gave rise to different signals, indicating restricted rotation about the phenyl–silicon bond (Tables 2 and 3).

All of the spectra were temperature dependent, and when the temperature was raised, coalescence phenomena of signals due to various diastereotopic groups could be observed. The four signals due to *N*-methyl groups coalesced into one singlet in both ^{13}C and ^1H NMR spectra (Tables 2 and 3), indicating that exchange between methyl groups takes place in a topomerization

(18) Klebe, G.; Qui, D. T. *Acta Crystallogr.* **1984**, *C40*, 476.

Table 4. Calculated Rate Constants and Free Energies of Activation for Exchange in **1**–**3** in Toluene-d_8 Solution and for **4** in Nitrobenzene-d_5

compd	X	R	temp,[a] K	$k_{12} = k_{34}$,[b] s^{-1}	$k_{13} = k_{24}$,[b] s^{-1}	$k_{14} = k_{23}$,[b] s^{-1}	ΔG_1*,[c] kcal/mol	ΔG_2*,[c] kcal/mol	ΔG_1*,[d] kcal/mol
1a	H	Me	340	0	27	82	17.0	17.8	16.5(C*Me*)
1b	H	Ph	345	0	60	14	17.5	18.5	
1c	H	CF_3	345	0	60	30	17.5	18.0	
2a	Me	Me	280	0	96	16	13.8	14.8	
2b	Me	Ph	285	0	100	13	13.7	14.8	
2c	Me	CF_3	283	0	162	32	13.7	14.6	13.8(CF_3)[e]
3a	Ph	Me	337	280	0	70	15.9	16.9	15.8(C*Me*)
3b	Ph	Ph	337	330	0	165	15.8	16.4	15.8(*ortho* H)
3c	Ph	CF_3	335	300	0	150	15.9	16.3	15.4(*ortho* H)
3d	Ph	CH_2Ph	335	280	0	70	15.9	16.9	15.8(*ortho* H)
4a[d,f]	Cl	Me	346	11			17.9		
4b[d,f]	Cl	Ph	363	13			19.5		
4c[d,f]	Cl	CF_3	393	26			20.7		

[a] Temperatures near the coalescence at which the corresponding rate constants were obtained by spectrum simulation. [b] The numerical indices correspond to the order of N–Me singlets, from high to low δ values. [c] Free energies of activation obtained from the given temperature and corresponding calculated rate constant using Eyring's equation, derived from the *N*-methyl signals. Rate constants were calculated by spectrum simulation. Barriers are estimated to be accurate within 0.2 kcal/mol. [d] Barriers at the coalescence temperature of indicated groups, from coalescence rate constants calculated by the equation $k_c = 2.22\Delta\nu_c$.[21] [e] Free energies of activation obtained from ^{19}F NMR (JEOL FX90Q). [f] Measured at 90 MHz, in nitrobenzene-d_5 solution. Due to the higher symmetry only two *N*-methyl singlets and a single coalescence process are observed.

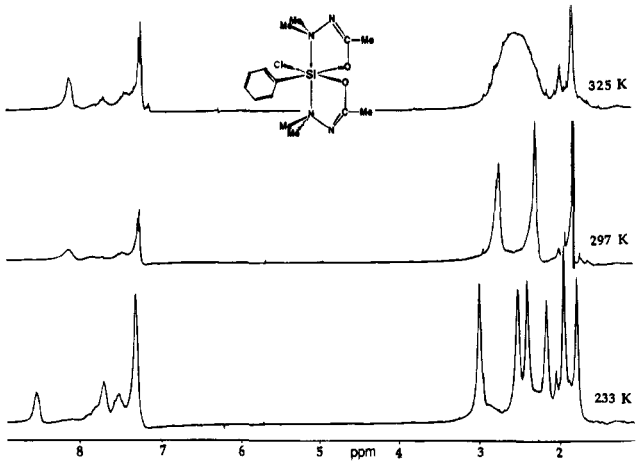

Figure 2. ^1H DNMR spectra for the exchange processes of **3a** in acetone-d_6.

reaction. Complete line shape analysis[19] for the exchange of the *N*-methyl proton signals among the four chemical sites showed that a set of six equal rate constants was insufficient to fully describe the process. At first simulations were achieved with two sets of equal rate constants, four in one set and two in the other. However, better fits to the experimental spectra were obtained when three pairs of rate constants were used: a pair of zero rate constants and two pairs of different, finite constants, as shown in Table 4. These results indicate that exchange takes place in two different rate processes. The energy barriers for the two processes in this solvent were quite close, and could only be detected by spectrum simulation.

Two distinct and separate rate processes were observed in **1a**–**c** and **3a**–**d** when the spectra were run in other solvents, dichloromethane-d_2 or acetone-d_6 (Figure 2).[20] The two barriers were immediately evident from the observation of two separate coalescence phenomena at different temperatures: the four *N*-methyl singlets observed at the slow echange limit temperature first coalesced into two singlets, which upon further heating coalesced again to one singlet. The observation that these rate processes were fully resolved and separated in dichloromethane-d_2 and acetone-d_6 solvents, as opposed to their combined appearance in toluene-d_8 solution, led to a more detailed study of the solvent dependence of activation barriers for one of the complexes, **3b**.

Table 5. Solvent Effect on Activation Free Energies for Exchange in **3b**[a]

solvent	signal	no. of signals at 300 K	T_c, K	ΔG_1*,[b] kcal/mol	ΔG_2*,[b] kcal/mol
CCl_4	NMe	4	340	16.4	16.9
	ortho H	2	350	16.4	
$CD_3C_6D_5$	NMe	4	337	15.8	16.4
	ortho H	2	340	15.8	
C_6D_6	NMe	4	340	16.3	16.7
	ortho H	2	350	16.4	
C_4Cl_6	NMe	4	345	16.6	16.9
	ortho H	2	355	16.6	
C_5D_5N	NMe_{12}	2	292	13.9	
	NMe_{34}	2	280	14.0	
	NMe	2	340		16.1
	ortho H	2	300	14.0	
$C_6D_5NO_2$	NMe_{12}	2	270	13.2	
	NMe	2	340		16.2
	ortho H	2	280	13.1	
$(CD_3)_2CO$	NMe_{12}	2	278	13.8	
	NMe_{34}	2	286	13.7	
	NMe	2	315		15.0
	ortho H	2	296	13.8	
$CDCl_3$	NMe	2	325		15.5
CD_2Cl_2	NMe_{12}	2	216	10.6	
	NMe_{34}	2	230	10.9	
	NMe	2	315		15.0
CD_3NO_2	NMe_{12}	2	<240	~10.6	
	NMe	2	335		16.0

[a] Where *N*-methyl signals appear as two singlets, rate constants were estimated at the coalescence temperature ($k_c = 2.22\Delta\nu$)[21] and barriers calculated using Eyring's equation; in cases of four singlets the rate constants were extracted from spectrum simulation, and used for calculating barriers at given temperatures for interchange between given signals. [b] Free energies of activation are estimated to be accurate to within 0.2 kcal/mol.

The spectra for **3b** were run in different solvents (Table 5). The table clearly demonstrates a strong solvent effect on activation barriers. The solvents studied may be divided into three groups. The first group includes the apolar solvents toluene-d_8, benzene-d_6, CCl_4, and hexachlorobutadiene, in which both activation barriers are relatively high and the corresponding spectral changes occur simultaneously and are observed only by line shape analysis. A second group of solvents consists of

(19) Line shape analysis was made using a PC computer and a local program based on the equations by G. Binsch (*Top. Stereochem.* **1968**, *3*, 97).

(20) However, for compounds **2** in these solvents the *N*-methyl signals were not fully resolved.

(21) Kost, D.; Carlson, E. H.; Raban, M. *J. Chem. Soc., Chem. Commun.* **1971**, 656.

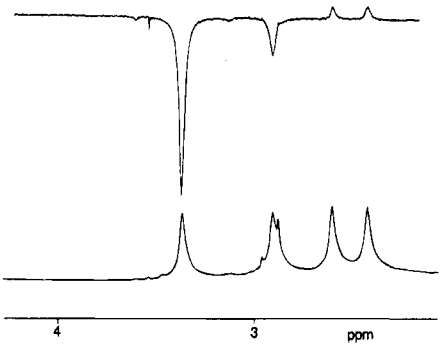

Figure 3. NOE and saturation transfer difference spectrum for **3b** in acetone-d_6 solution at 240 K. The *N*-methyl region is shown. The upper trace shows the difference spectrum (the low-field singlet was saturated prior to the observation pulse); the lower trace shows the reference spectrum.

the more polar acetone-d_6, nitrobenzene-d_5, and pyridine; in these solvents the *N*-methyl groups appear as two singlets at room temperature, and the two barriers are well separated and directly observed. The third group includes chloroform-d_1, dichloromethane-d_2, and nitromethane-d_3, whose lower barriers are substantially lower (up to 5 kcal mol^{-1}) than those measured in apolar solvents. Other complexes showed NMR behavior similar to that described here for **3b**, i.e., two separate exchange processes.

In addition to the *N*-methyl exchange phenomena, *C*-methyl coalescence is found in Figure 2 at the high-field end of the spectrum of **3a**, simultaneously with the first (lower temperature) *N*-methyl exchange. The simultaneous exchange of *C*-methyl and *N*-methyl signals indicates that the first (lower barrier) rate process is associated with the exchange of the two chelate rings; i.e., no coalescence of geminal *N*-methyl signals takes place in this process. Direct evidence for this was obtained for **3b** in the following difference NOE-and-saturation-transfer experiment (Figure 3).

The ^{1}H NMR spectrum of **3b** in acetone-d_6 solution at 240 K shows four *N*-methyl signals. At this temperature selective low-power irradiation at each *N*-methyl site causes substantial saturation transfer to the site of first exchange, but no detectable saturation transfer due to the slower rate process. A small but significant positive nuclear Overhauser enhancement is observed to the other sites, which do not interchange with the irradiated sites (Figure 3). Since NOE is not possible between *N*-methyl signals on different chelate rings, due to the substantial distance, one of the positive signals must be due to the geminal neighbor of the irradiated methyl group. This is evidence that the geminal methyl neighbors (connected by NOE signals) do not exchange at this temperature, and hence undergo exchange only at the second, slow process. It is therefore concluded that the lower energy exchange renders the two chelate rings equivalent, and hence is associated with their interchange.

The observed coalescence associated with the exchange of the *ortho* protons and carbons in the phenyl ring attached directly to silicon in complexes **3** was also found to be associated with the lower energy exchange process, interchanging the two diastereotopic chelate rings (Figure 2, Table 5).

The effect of the concentration of the complexes on the barriers has been studied. In all cases the barriers were found to be essentially independent of concentration (upon 8-fold dilution), and hence bimolecular processes might be excluded.

To enable further stereochemical analysis, compound **3d**, in which the ring substituent is the prochiral benzyl group, was prepared: if the first (lower) barrier involves complete enantiomer interconversion, the initial two AB quartets expected at

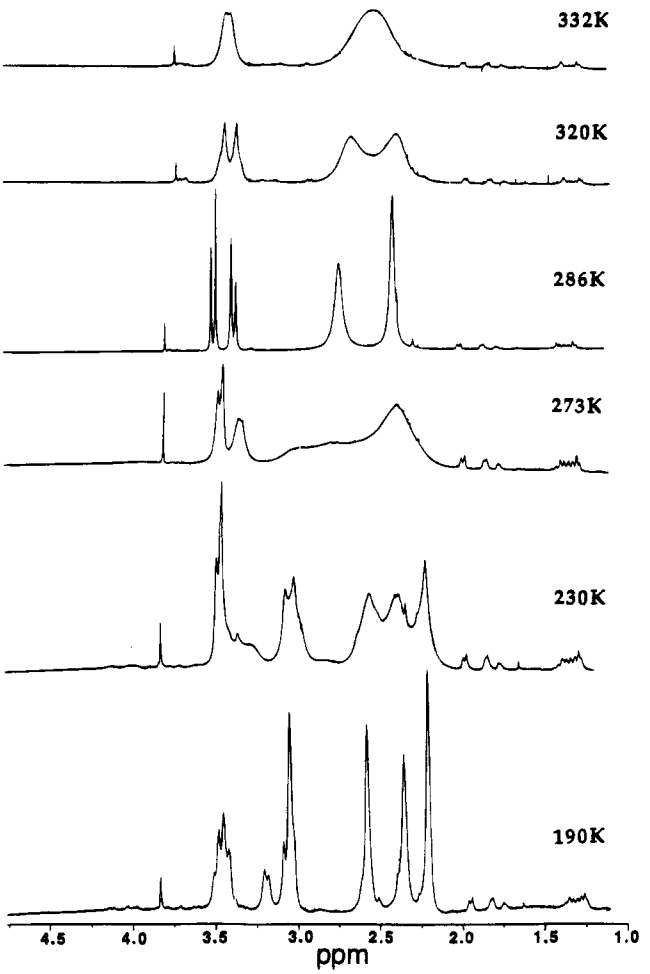

Figure 4. Variable temperature NMR spectra of **3d** in CD_2Cl_2 solution (500 MHz). The *N*-methyl and benzyl methylene regions are shown. The low-temperature resolution of the methylene quartets is limited, but initial coalescence to one AB quartet is clearly seen, followed by coalescence of the quartet to a singlet.

the slow exchange temperature would coalesce into two *singlets*, which, upon a further increase in temperature, would coalesce to one singlet. Conversely, initial coalescence of the AB quartets into a single quartet, followed by coalescence into a singlet, would mean that signals due to protons on *different* benzyl groups exchange first, while geminal protons remain nonequivalent.[22] The variable temperature ^{1}H NMR spectra of **3d** (Figure 4) clearly display initial coalescence of the benzyl methylene protons into one quartet, and provide evidence that complete enantiomerization with exchange of geminal groups does *not* take place in the first rate process. Table 6 lists the rate constants and activation barriers obtained for **3d**.

3.b. Discussion. The results presented above permit a limited topological and mechanistic analysis of the exchange processes. The key observation is the existence of *only one* isomer in solution. Thus, any exchange mechanism under consideration must account for topomerization, i.e., transformation of the observed isomer to itself, associated with interconversion of diastereotopic groups within the same species.

From a purely topological point of view, there are 720 (6!) permutations by which six ligands can be arranged about a central atom in an (idealized) octahedral geometry.[23] For complexes of type M(AB)(CD)XY imposition of the constraint that bidentate ligands cannot assume *trans* positions reduces

(22) For a similar analysis in a different molecular system see: Kost, D.; Egozy, H. *J. Org. Chem.* **1989**, *54*, 4909. Kost, D.; Zeichner, A.; Sprecher, M. S. *J. Chem. Soc., Perkin Trans. 2*, **1980**, 317.

Table 6. Dynamic NMR Data for Exchange in **3d** (CD_2CL_2)

signal	$\Delta\nu$, Hz	T_c, K	ΔG_1^* kcal/mol	ΔG_2^* kcal/mol
CH_2 (1 ⇌ 3)[a]	45	232	11.2	
CH_2 (2 ⇌ 4)[b]	72	232	11.1	
NMe (1 ⇌ 3)[b]	73	236	11.3	
NMe (2 ⇌ 4)[b]	170	243	11.3	
CH_2 (1,3 ⇌ 2,4)	33	315		15.6
NMe (1,3 ⇌ 2,4)	61	317		15.5

[a] The apparent exchange is between the low-field half of one quartet (labeled 1) and the low-field half of the other (3), and between the high-field half of one quartet (2) and the high-field half of the other (4). The low-temperature spectra were not sufficiently resolved to permit accurate determination of $\Delta\nu$ and T_c for these signals, and hence the uncertainty in these data should be taken as 30% and 4 °C, respectively. [b] Coalescence of signals 1 with 3 (in order of increasing field) and of 2 with 4 is observed.

the number to 480. Elimination of all the permutations which are related by rotations of the whole molecule, represented by the four C_3 and three C_4 rotational axes of the octahedral skeleton (total of 24), reduces the number further to 20. When CD = AB [$M(AB)_2XY$], the interchange of AB pairs reduces the number of isomers further to 10. However, for structure **I** (Figure 1) this AB ⇌ AB interchange is equivalent to a C_2 rotation, which has already been accounted for. The final number of independent isomers (including enantiomers) is therefore 11, represented by the six diastereomers of Figure 1.

The only observed transformations are topomerizations of the one existing stereoisomer, depicted above for **1**–**4** (**IV** in Figure 1). All the other transformations, leading from one diastereomer to another, may be excluded. Topologically only three exchange processes are allowed, which constitute true topomerizations and may lead from this stereoisomer to its topomers: exchange of X with Cl, exchange of the two oxygen atoms, and exchange of the nitrogens.

The above analysis relates only to the initial and final molecular geometries, but provides no information on the actual mechanism by which these transformations take place. We now turn to analyze the results in light of possible exchange reaction pathways.

Several different mechanisms have been proposed in the literature to account for the dynamic behavior of silicon and other hexacoordinate organometallic chelates.[2] These include two main groups: dissociative[7] (inter- or intramolecular) and nondissociative (intramolecular)[8a] processes. Within the dissociative processes, one could envision dissociation of a monodentate ligand or one side of a bidentate ligand to produce a pentacoordinate intermediate, which, in turn, could either exchange *via* pseudorotation[24] or exchange *via* return of the leaving ligand to a different location. Dissociation of two ligands (or a bidentate ligand) has also been considered.[7]

The nondissociative stereomutations (topomerizations or diastereomerizations) can also proceed in several ways: the Bailar[25] and Ray–Dutt[26] twists, in which one triangular face of the idealized octahedron rotates relative to the opposite face, through a trigonal prism transition state, or a direct 1,2-exchange of ligands, *via* the so-called "bicapped tetrahedron" transition state or intermediate.[27]

Dissociative Exchange. The observed independence of exchange rates upon the concentration of the chelates is evidence that no intermolecular process takes place. The only other dissociative process left as an option is an intramolecular dissociation–recombination reaction within the "solvent cage". The most likely ligand to dissociate would be one of the dimethylamino groups, which is bound to silicon by a dative (and not fully covalent) bond. However, the evidence presented below rules out this possibility.

The results of the dynamic NMR study of **3d** (Table 6) indicate that no silicon–nitrogen dative bond cleavage takes place during the exchange processes. It was found that benzyl coalescence to a singlet and *N*-methyl coalescence occurred *simultaneously* with the same activation free energy (Table 6, Figure 4). However, since Si–N bond cleavage and the resulting exchange of geminal *N*-methyls (by rotation about the N–N bond) would *not* cause a concomitant exchange of the geminal methylene protons, it may be concluded that both of these exchanges take place by a different mechanism, and that Si–N bond cleavage does *not* occur and may be excluded on this time scale. This conclusion supports a nondissociative process.

We may consider Si–Cl bond dissociation and recombination. To solve this problem, we prepared the fluoro complex **18**, by reacting $PhSiF_3$ in place of $PhSiCl_3$ with *O*-(trimethylsilyl)-*N*,*N*-dimethylbenzohydrazide, **6b**. The octahedral geometry of **18** and analogy to the chloro complexes are established by two observations: (a) the ^{29}Si chemical shift for **18** (δ = −148.6 ppm) is well within the range of octahedral hexacoordinate complexes. (b) **18** behaves in full analogy to **1**–**4** as far as stereodynamics are concerned; in its proton and ^{13}C spectra the usual pattern of *N*-methyl signals appears (four singlets in $CDCl_3$ solution), which, upon a temperature increase, undergo coalescence to a singlet (coalescence temperature for the ^{13}C spectrum, 340 K), as do the *ortho* phenyl carbons.

18 has a direct bond between silicon and fluorine, and hence strong $^{29}Si-^{19}F$ coupling is observed in the ^{29}Si NMR spectrum (^1J(Si–F) = 272.9 Hz). However, neither $^{29}Si-^{19}F$ coupling nor $^{19}F-^{13}C$ coupling observed for the *ipso* carbon of the Si–phenyl ring (J = 43.6 Hz) collapses upon heating. This proves that no fluorine exchange takes place during the process which interconverts the other pairs of diastereotopic groups: *N*-methyls and *ortho* protons and carbons.

It might be argued that the absence of Si–F bond dissociation is not evidence for the analogous persistence of the Si–Cl bond in **1**–**4**. However, the fact that in **18** all other exchanging groups undergo coalescence at comparable temperatures and barriers as the corresponding groups in the chloro complexes shows that the fluoro and chloro compounds behave similarly, i.e., undergo the same exchange processes. Therefore, it must be concluded that also in the chloro compounds exchange does not involve Si–Cl dissociation, since the mechanisms are analogous.

The evidence thus rules out a dissociative mechanism for the observed exchange phenomena. In the next section we propose a nondissociative process, compatible with all the observations.

Nondissociative Exchange. Of the multitude of exchange mechanisms which have been observed or postulated in various chelate systems, we propose the one which can best account for all of the observations, while remaining simple and compact. This exchange mechanism is the direct, intramolecular 1,2-shift (sometimes also referred to as "crossover")[28] of adjacent ligands through a "bicapped" tetrahedral transition state or intermediate, as depicted in Figure 5. The exchange takes place by a twist of two ligands out of the equatorial plane to form a tetrahedron-like geometry, while the two axial ligands bend away from the

(23) For permutational analyses of similar chelates see: (a) Bickley, D. G.; Serpone, N. *Inorg. Chem.* **1976**, *15*, 948. (b) Pignolet, L. H. *Top. Curr. Chem.* **1975**, *56*, 91.

(24) Berry, R. S. *J. Chem. Phys.* **1960**, *32*, 933.

(25) Bailar, J. C., Jr. *J. Inorg. Nucl. Chem.* **1958**, *8*, 165.

(26) Ray, P.; Dutt, N. K. *J. Indian Chem. Soc.* **1943**, *20*, 81.

(27) Hoffmann, R.; Howell, J. M.; Rossi, A. R. *J. Am. Chem. Soc.* **1976**, *98*, 2484.

(28) Rodger, A.; Johnson, B. F. G. *Inorg. Chem.* **1988**, *27*, 3061.

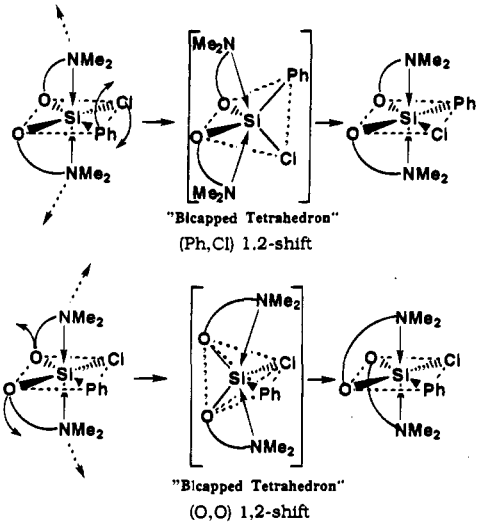

Figure 5. 1,2-Shift mechanism of topomerization *via* a bicapped tetrahedron intermediate or transition state: (upper part) phenyl–chlorine interchange; (lower part) oxygen–oxygen interchange.

exchanging groups with a considerable increase in their bond lengths to silicon (up to 32%, according to an analysis by Rodger and Johnson).[28] The 1,2-shift mechanism can directly effect two of the three topomerizations discussed above: exchanges of the (X, Cl) and (O, O) ligand pairs, respectively. The third topological process which is associated with a topomerization, the (N, N) exchange, cannot take place by this mechanism, since the interconverting ligands are in a *trans* geometry. The 1,2-shift mechanism thus provides two similar exchange pathways, which may account for the observation of two rather close exchange barriers.

The bicapped tetrahedron geometry is strongly supported by the results obtained by Corriu and co-workers:[12] some of their hexacoordinate silicon complexes were shown by X-ray crystallography to have this geometry *in the ground state*. It is thus evident that this can be a stable structure even relative to the octahedral geometry, and undoubtedly can be stable enough to be a likely intermediate in the exchange reaction, or at least a reasonable low-energy transition state. Hoffmann *et al.* also discussed the bicapped tetrahedral geometry as a possible structure for hexacoordinate complexes and exchange intermediates.[27] This geometry has been considered a transition state in a photochemical exchange reaction.[29]

Preliminary molecular orbital calculations at the semiempirical level seem to qualitatively support the stability of the bicapped tetrahedron geometry:[30] interestingly, geometry optimization using PM3 parametrization[31] of the C_1 complex **18** converged to a nearly octahedral geometry, whereas optimization of the same molecule at the ZINDO1[32] level led to the bicapped tetrahedral geometry. Further ab initio calculations are underway to resolve this conflict.

Examination of the two exchanges (O, O) and (X, Cl) reveals that they precisely effect the observed spectral behavior: (X, Cl) interchange equilibrates the two chelate rings, and thus is associated with coalescence of signal pairs due to diastereotopic groups residing on different rings. The second process, (O, O) exchange, brings about a similar exchange of chelate rings, and

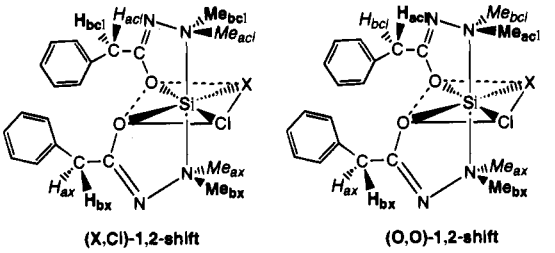

Figure 6. Exchange relationships between diastereotopic groups in **3d** associated with each of the two 1,2-shift mechanisms. Pairs of interchanging groups are identified by italic or bold labels.

in addition inverts their helical arrangement. The effect of these 1,2-shifts may best be viewed with respect to the dibenzyl compound **3d** (Figure 6). The two chelate rings can be distinguished by the fact that the oxygen of one of the rings is opposite (*trans* to) chlorine, while that of the other ring is opposite the X group. The four benzyl methylene protons are initially diastereotopic, at the slow exchange limit temperature, and may be labeled H_{ax}, H_{bx}, H_{acl}, and H_{bcl}, according to the group (X or Cl) *trans* to the corresponding chelate ring. H_{ax} and H_{bx} differ in that the proton labeled a points (on average) toward the other chelate ring, whereas the one labeled b points away from the other ring (see Figure 6).

It is evident from Figure 6 that the (X, Cl)-shift interchanges H_{ax} with H_{acl} and H_{bx} with H_{bcl}, while the (O, O)-shift interchanges H_{ax} with H_{bcl} and H_{acl} with H_{bx}. Note that neither of these stereomutations exchanges geminal protons, H_{ax} with H_{bx} or H_{acl} with H_{bcl}. It is only the combination of *both* processes that eventually causes coalescence of signals due to geminal protons (and *N*-methyl groups). Indeed, the faster of the two observed rate processes involves exchange and equilibration of the two chelate rings, i.e., $H_{ax} \rightleftarrows H_{acl}$ or $H_{ax} \rightleftarrows H_{bcl}$ in **3d**, as well as nonadjacent *N*-methyl groups in other compounds of the series, as shown by the NOE experiment, and simultaneous exchange of *C*-methyl groups and chelate ring carbons. The second (higher energy) process is compatible with loss of chirality of the compounds, since the AB quartet of the prochiral benzyl protons coalesces to a singlet (Table 6). In this case also the *N*-methyl coalescence occurs simultaneously, as required by the 1,2-shifts. Since *both* exchanges are required to bring about a complete enantiomerization, the above information is still insufficient to determine which of the two 1,2-shifts corresponds to the lower and which to the higher energy process.

This dilemma may perhaps be resolved by reference to the coalescence of the *ortho* groups (protons and carbons) of the Si–phenyl ring in **3**. Evidently rotation of this ring about the Si–C bond is restricted at the ground state conformation, causing the *ortho* groups to be diastereotopic. Examination of models shows that during (Ph, Cl)-1,2-shift, the phenyl may undergo correlated rotation, such that the *ortho* protons exchange positions. As a result, when this process becomes rapid relative to the NMR time scale, the signals due to the *ortho* groups coalesce. By contrast, the 1,2-shift of the oxygen atoms has little effect on the position of the phenyl ring, and hence neither causes similar correlated rotation, nor relieves the restriction on free rotation. It may therefore be argued that since the lower energy barrier brings about, among other groups, exchange of the *ortho* groups, this process may be assigned the (Ph, Cl)-1,2-shift.

During the 1,2-shift a significant increase in the Si–N bond length must occur, although, as the evidence presented above indicates, complete Si–N bond cleavage does not occur. The expected increase in the dative bond lengths in the transition state is confirmed and supported by two observations: (a) the

(29) Burdett, J. K. *Inorg. Chem.* **1976**, *15*, 212.
(30) Kost, D.; Kalikhman, I. D. Unpublished results.
(31) Stewart, J. J. P. *J. Comput. Chem.* **1991**, *12*, 320. Stewart, J. J. P. *J. Comput. Chem.* **1989**, *10*, 209. Stewart, J. J. P. *J. Comput. Chem.* **1989**, *10*, 221.
(32) Bacon, A. D.; Zerner, M. C. *Theor. Chim. Acta* **1979**, *53*, 21. Anderson, W. P.; Edwards, W. D.; Zerner, M. C. *Inorg. Chem.* **1986**, *25*, 2728.

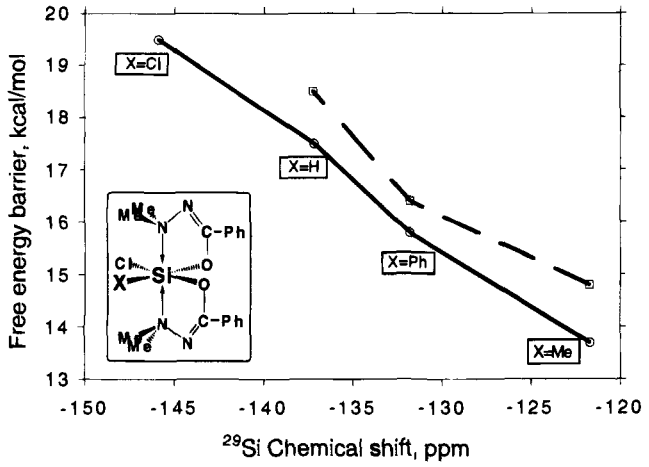

Figure 7. Free energies of activation for both barriers in compounds **1b**–**4b** (in toluene-d_8) as a function of ^{29}Si chemical shift (in $CDCl_3$).

solvent dependence of the barriers (Table 5) and (b) the correlation of barrier heights with ^{29}Si chemical shifts (Figure 7).

A remarkable effect of solvent on the barrier heights was found. The variation in barriers as a function of solvent did not follow any simple solvent polarity parameter. Rather, solvents which are hydrogen bond donors ($CDCl_3$ and CD_2Cl_2) and those which are powerful electron acceptors (deuterionitromethane and nitrobenzene) accelerate the exchange reaction. This suggests that association of a solvent molecule with the basic dimethylamino ligand assists the exchange reaction by weakening the N → Si dative bond, and facilitating the bond length increase necessary for the 1,2-shift.

The second observation which may be related to an increase in the Si–N bond length in the transition state is the linear correlation found between each of the barriers and the corresponding ^{29}Si chemical shifts (Figure 7). We consider the increase in ^{29}Si chemical shifts a result of the increase in the electronegativity of the X ligand group.[33] It follows therefore that the barriers increase with increasing electronegativity of the X ligand. This can be explained as follows: the more electronegative ligand causes stronger binding (i.e., shorter bonds) of all ligands to silicon. Thus, a larger Si–N bond length increase is necessary in the presence of a more electronegative X ligand in order to facilitate the 1,2-shift. As a result the barrier observed in the presence of an electronegative ligand X is higher than the one observed in the presence of a less electronegative ligand.

A variant of the bicapped tetrahedral exchange mechanism is one in which the 1,2-shift occurs *nonsymmetrically*, i.e., with only one of the Si–N dative bonds extending, and a transition state which resembles a pentacoordinate more than a bicapped tetrahedral geometry. These two mechanisms are indistinguishable experimentally, and the arguments for the latter are (a) it would be easier (lower barrier) to cleave or extend one Si–N bond than two and (b) the resulting nearly trigonal bipyramidal intermediate is likely to topomerize via a 1,2-shift. The main argument in favor of the bicapped tetrahedron (symmetrical) exchange is the discovery of stable structures of this kind.

Within the nondissociative mechanisms two well-documented exchange reactions are the Bailar[25] and Ray–Dutt (R–D)[26] twist mechanisms (Figures 8 and 9). Each of these exchange mechanisms converts the predominant diastereomer to a *different diastereomer*, and thus cannot account for the observed topomerizations. A single Bailar or Ray–Dutt twist may thus be ruled out as a possible exchange mechanism. However, a closer examination (Figures 8 and 9) reveals that two consecutive twists of the Bailar and R–D types can be found which are, in fact, stereochemically equivalent to the (X, Cl)- and (O, O)-1,2-shifts (i.e., they bring about the same exchange between two permutants of the same diastereomer). This possibility, of two consecutive twist motions to account for each of the observed topomerizations, cannot be ruled out by the available data. However, we favor the 1,2-shift mechanism, for the following reasons: (a) Two processes must be invoked for each topomerization, whereas the 1,2-shift mechanism is a single process for each observed rate process, which accounts for the results in a simple straightforward manner. (b) Since there are many possible twist sequences that lead to the observed topomerizations, and since the two twist mechanisms (R–D and Bailar) are very similar in their steric requirements, it would be difficult to argue why these processes lead to the observation of *two different* exchange barriers. (c) Perhaps the strongest argument in favor of the direct shift mechanism is the proven stability of the bicapped tetrahedral structures in analogous hexacoordinate silicon chelates *in the ground state*. This fact makes the bicapped tetrahedron a very likely transition state (or intermediate) and supports the 1,2-shift mechanism. The alternative twist mechanisms must go through a trigonal prism transition state, which, in contrast, has not been observed in silicon chelates and may be assumed higher in energy.

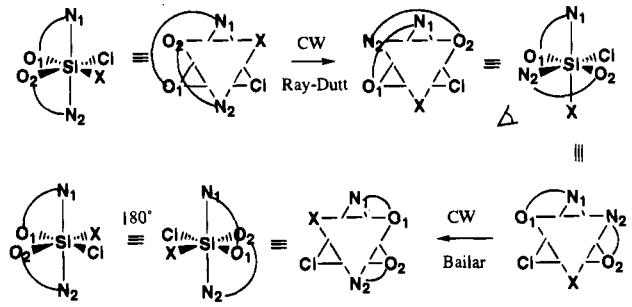

Figure 8. A Ray–Dutt twist followed by a Bailar twist, applied schematically to a model complex like **1**–**3**. Each of the two processes exchanges diastereomers, but the combined action is a topomerization equivalent to a (X, Cl)-1,2 shift. The "eye" drawn near one of the structures shows which triangular face was selected for the second twist process.

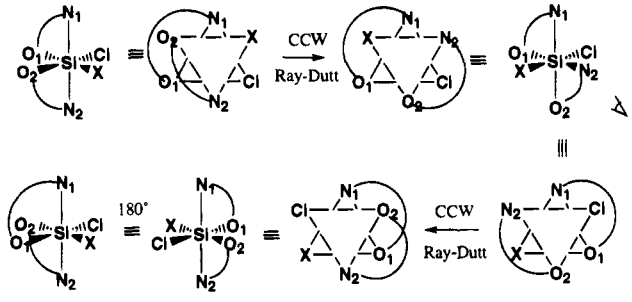

Figure 9. Two consecutive Ray–Dutt twists applied schematically to a model complex like **1**–**3**. While each of the two processes exchanges diastereomers, the combined action is topologically equivalent to an (O, O)-1,2 shift. The "eye" drawn near one of the structures shows which triangular face was selected for the second twist process.

4. Experimental Section

All the reactions were carried out under dry nitrogen or argon. NMR spectra were obtained using a Bruker WP-200-SY spectrometer operating at 200 MHz for protons, unless otherwise stated. ^{13}C and ^{29}Si NMR spectra were recorded with broad-band proton decoupling,

(33) This is evident from the fact that these chemical shifts also correlate linearly with the corresponding ^{29}Si chemical shifts of the tetravalent silicon chloride analogues $XSiCl_3$ (slope, 1.2476; correlation coefficient, 0.9878).

using the INEPT pulse sequence for ^{29}Si spectra. Chemical shifts are reported in parts per million relative to internal tetramethylsilane (δ). The temperatures were controlled by a Bruker VT-1000 temperature control unit, and were calibrated using methanol or ethylene glycol spectra as needed for low and high temperatures, respectively. The temperatures are considered to be accurate to within 2 °C.

The NOE-and-saturation-transfer experiment was performed using a microprogram which selectively irradiated each singlet for 3 s at low power, followed by a 90° acquisition pulse. The acquired FID was subtracted from a reference FID, obtained under the same conditions with the CW irradiation off resonance. The difference FID was Fourier transformed to produce the reported spectrum. Eighty scans were accumulated for each of the irradiated and reference spectra.

Mass spectra (low-resolution, isobutane, CI) were measured on a Finnigan TSQ-70B instrument. High-resolution mass spectra (70 eV, EI) were obtained using a Finnigan MAT-711 HRMS. Elemental analyses were performed at the Analytical Laboratory, Institute of Organic Chemistry, Siberian branch of the Russian Academy of Science, Irkutsk.

O-trimethylsilylated 1,1-dimethyl-2-acylhydrazines **6a**–**c** were prepared as described previously,[34] and distilled under reduced pressure. The boiling points were as follows: **6a**, 51–52 °C (30 mmHg), lit.[34a] 45 °C (20 mmHg); **6b**, 80–82 °C (0.8 mmHg), lit.[34b] 110–112 °C (2 mmHg); **6c**, 70–73 °C (30 mm), lit.[34c] 41 °C (10 mmHg).

O-trimethylsilylated 1,1-dimethyl-2-(phenylacetyl)hydrazine (6d) was prepared by the same method, reaction of Me_3SiCl with *N,N*-dimethylphenylacetohydrazide: bp 56–57 °C (0.2 mmHg); ^1H NMR ($CDCl_3$) δ 2.34, 2.36 (2s, (*Z,E*)-NMe_2, 6H), 3.40, 3.81 (2s, (*Z,E*)-CH_2, 2H), 0.22, 0.08 (s, (*Z,E*)-Me_3Si, 9H); ^{13}C NMR ($CDCl_3$) δ 0.2, 0.4 ((*Z,E*)-Me_3Si), 35.1, 41.6 ((*Z,E*)-CH_2), 46.6, 48.3 ((*Z,E*)-NMe_2), 124.0–136.6 (Ph), 158.9, 156.2 ((*Z,E*)-C=N); ^{29}Si NMR ($CDCl_3$) 18.1, 20.4 ((*Z,E*)-isomers). Anal. Calcd for $C_{13}H_{22}N_2OSi$: C, 62.36; H, 8.86; N, 11.20. Found: C, 61.66; H, 8.78; N, 11.07.

Bis(*N*-(dimethylamino)acetimidato-*N,O*)chlorohydridosilicon-(IV) (1a). A mixture of 1.75 g (0.01 mol) of **6a** and 0.68 g (0.005 mol) of trichlorosilane (**7**) was stirred under vacuum in 20 mL of dry CH_2Cl_2 for 1 h at 25 °C, followed by removal of solvent under reduced pressure (0.3 mmHg). 1.3 g (97% yield) of colorless crystals were obtained: mp 135–137 °C; ^1H NMR ($CDCl_3$) δ 1.88 (s, 6H, CMe), 2.90 (s, 12H, NMe_2), 5.13 (s, 1H, SiH); ^{13}C NMR ($CDCl_3$) δ 17.6 (Me), 49.9, 50.5 (NMe_2), 167.2 (C=N); HRMS for M^+ ($C_8H_{19}ClN_4O_2Si$), calcd 266.0966, found 266.0976.

1b and **1c** were prepared by the same method as **1a**, and were obtained in essentially quantitative yields. Attempts to recrystallize **1a**–**c** resulted in decomposition, presumably by disproportionation, leading to **4a**–**c**. Characterization of **1b** and **1c** is based on the analogy in NMR spectra.

Bis(*N*-(dimethylamino)benzimidato-*N,O*)chlorohydridosilicon-(IV) (1b): mp 92–95 °C; ^1H NMR ($CDCl_3$) δ 3.13 (s, 6H, NMe_2), 3.24 (s, 6H, NMe_2), 5.30 (s, 1H, SiH), 7.3–7.9 (m, 12H, Ph); ^{13}C NMR ($CDCl_3$) δ 50.4, 50.9 (NMe_2), 127–133 (Ph), 165.0 (C=N).

Bis(*N*-(dimethylamino)trifluoroacetimidato-*N,O*)chlorohydridosilicon(IV) (1c): mp 112–116 °C; ^1H NMR ($CDCl_3$) δ 3.00 (s, 3H, NMe_2), 2.96 (s, 3H, NMe_2), 2.83 (s, 3H, NMe_2), 2.81 (s, 3H, NMe_2), 5.12 (s, 1H, SiH); ^{13}C NMR ($CDCl_3$) δ 51.1, 50.6, 49.7, 49.0 (NMe_2), 127–133 (Ph), 156.4 (q, C=N, ^2J(C–F) = 39.0 Hz), 157.3 (q, C=N, ^2J(C–F) = 39.0 Hz), 116.5 (q, CF_3, ^1J(C–F) = 279 Hz); HRMS for M^+ ($C_8H_{13}ClF_6N_4O_2Si$), calcd 374.0400, found 374.0372; LRMS (CI) *m/z* (relative intensity, ion) 375.1 (11, $M^+ + 1$), 339.1 (5, $M^+ - Cl$), 157.1 (100, $CF_3CONHNMe_2 + 1$).

Bis(*N*-(dimethylamino)phenylacetimidato-*N,O*)chloro(methyl)silicon(IV) (2b). A solution of 2.54 g (0.0108 mol) of **6b** and 1.0 g (0.0067 mol) of methyltrichlorosilane (**8**) in 20 mL of dry CH_2Cl_2 was magnetically stirred for 8 h at 20 °C in an evacuated ampule. The solvent was evaporated under reduced pressure (0.3 mmHg). Recrystallization of the residue from 50 mL of hexane gave 1.96 g of **2b** (75% yield), colorless crystals with mp 132.5–133.5 °C: ^1H NMR ($CDCl_3$) δ 0.69 (s, 3H, SiMe), 3.15 (s, 12H, NMe_2), 7.3–7.8 (m, 10H, Ph); ^{13}C NMR ($CDCl_3$) δ 11.8 (SiMe), 51.6 (NMe_2), 163.6 (C=N), 127–134 (Ph); LRMS (CI) *m/z* (relative intensity, ion) 404.2 (5, $M^+ + 1$), 367.1 (5, $M^+ - Cl$). Anal. Calcd for $C_{19}H_{24}ClN_4O_2Si$: C, 56.49; H, 5.99; Cl, 8.78; N, 13.87; Si, 6.95. Found: C, 56.78; H, 6.36; Cl, 9.20; N, 13.33; Si, 6.82.

Bis(*N*-(dimethylamino)acetimidato-*N,O*)chloro(methyl)silicon-(IV) (2a). This complex was prepared as described for **2b**, and recrystallized from hexane to yield colorless crystals with mp 113–115 °C: ^1H NMR ($CDCl_3$) δ 0.67 (s, 3H, SiMe), 1.86 (s, 6H, CMe), 2.92 (s, 12H, NMe_2); ^{13}C NMR ($CDCl_3$) δ 9.8 (SiMe), 17.6 (CMe), 51.0 (NMe_2), 166.3 (C=N). HRMS for ($M^+ - Cl$) ($C_9H_{21}ClN_4O_2Si$), calcd 245.1434, found 245.1473.

Bis(*N*-(dimethylamino)trifluoroacetimidato-*N,O*)chloro(methyl)-silicon(IV) (2c). The complex was prepared as described for **2b**, and recrystallized from hexane. The yield (before recrystallization) was 92%. Colorless crystals of mp 119–120 °C were obtained: ^1H NMR ($CDCl_3$) δ 0.69 (s, 3H, SiMe), 3.15 (s, 12H, NMe_2), 7.3–7.8 (m, 10H, Ph); ^{13}C NMR ($CDCl_3$) δ 11.8 (SiMe), 51.6 (NMe_2), 163.6 (C=N), 127–134 (Ph). Anal. Calcd for $C_9H_{15}ClF_6N_4O_2Si$: C, 27.81; H, 3.89; F, 29.32; N, 14.41; Cl, 9.12. Found: C, 27.57; H, 3.93; N, 14.72; F, 29.53; Cl, 9.29.

Bis(*N*-(dimethylamino)acetimidato-*N,O*)chloro(phenyl)silicon-(IV) (3a). A mixture of 1.74 g (0.01 mol) of **6a**, 1.1 g (0.0052 mol) of phenyltrichlorosilane (**9**), and 20 mL of dry CH_2Cl_2 was stirred under vacuum for 2 h at 20 °C. The solvent was removed under reduced pressure. Recrystallization from 50 mL of hexane gave **3a** (1.3 g, 76% yield) as colorless crystals: mp 119–122 °C; ^1H NMR ($CDCl_3$) δ 1.92 (s, 6H, CMe), 2.34 (s, 6H, NMe_2), 2.80 (s, 6H, NMe_2), 8.04 (d, 2H, J = 8 Hz, SiPh *ortho* H), 7.3–7.8 (m, 3H, SiPh); ^{13}C NMR ($CDCl_3$) δ 17.3 (CMe), 51.0 (NMe_2), 166.0 (C=N), 127.6 (SiPh *meta* C), 128.4 (SiPh *para* C), 136.7 (SiPh *ortho* C), 142.4 (SiPh *ipso* C); LRMS (CI) *m/z* (relative intensity, ion) 342.9 (5, $M^+ + 1$), 307.2 (18, $M^+ - Cl$), 241.5 (5, $M^+ - Me_2NNMeCO$), 205.8 (100, $M^+ - Me_2NNMeCO - Cl$), 102 (83, $Me_2NNHCOMe^+$).

Compounds **3b** and **3c** were prepared by essentially the same method as **3a**.

Bis(*N*-(dimethylamino)benzimidato-*N,O*)chloro(phenyl)silicon-(IV) (3b). Crystallization from hexane afforded a 75% yield of colorless crystals: mp 159–161 °C; ^1H NMR ($CDCl_3$) δ 2.65 (s, 6H, NMe_2), 3.20 (s, 6H, NMe_2), 8.05 (d, 2H, J = 8 Hz, SiPh *ortho* H), 7.3–7.8 (m, 13H, Ph); ^{13}C NMR ($CDCl_3$) δ 51.7 (NMe_2), 164.0 (C=N), 137.9 (SiPh *ortho* C), 144.8 (SiPh *ipso* C), 126–146 (Ph); LRMS (CI) *m/z* (relative intensity, ion) 467.2 (5, $M^+ + 1$), 431.7 (100, $M^+ - Cl$), 165.0 (17).

Bis(*N*-(dimethylamino)trifluoroacetimidato-*N,O*)chloro(phenyl)-silicon(IV) (3c). Colorless crystals of **3c** were obtained upon crystallization from hexane: mp 125–130 °C; ^1H NMR ($CDCl_3$) δ 2.30 (s, 3H, NMe_2), 2.63 (s, 6H, NMe_2), 3.15 (s, 3H, NMe_2), 7.42 (d, 1H, J = 8 Hz, SiPh *ortho* H), 8.51 (d, 1H, J = 8 Hz, SiPh *ortho* H), 7.3–7.6 (m, 3H, Ph); ^{13}C NMR ($CDCl_3$) δ 51.2 (NMe_2), 156.9 (q, ^3J(C–F) = 35 Hz, C=N), 116.5 (q, ^1J(C–F) = 276.1 Hz, CF_3), 128.5 (SiPh *meta* C), 129.6 (SiPh *para* C), 135.7, 138.7 (SiPh *ortho* C), 141.7 (SiPh *ipso* C); LRMS (CI) *m/z* (relative intensity, ion) 451.1 (15, $M^+ + 1$), 415.6 (100, $M^+ - Cl$), 313, (45), 295.0 (37, $M^+ - Me_2NNCOCF_3$), 157 (50, $Me_2NNH_2COCF_3$).

Bis(*N*-(dimethylamino)phenylacetimidato-*N,O*)chloro(phenyl)silicon(IV) (3d). Colorless crystals were obtained upon crystallization from hexane: mp 96–98 °C; ^1H NMR ($CDCl_3$) δ 2.23 (s, 6H, NMe_2), 2.53 (s, 6H, NMe_2), 3.13 and 3.31, (d, 4H, ^2J = 14Hz, CH_2), 7.42 (d, 1H, J = 8 Hz, SiPh *ortho* H), 8.51 (d, 1H, J = 8 Hz, SiPh *ortho* H), 7.3–7.6 (m, 13H, Ph); ^{13}C NMR (toluene-d_8) δ 38.3 (CH_2), 50.4, 51.0, 51.9 (NMe_2), 166.8 (C=N), 136.0, 138.9 (*ortho* C), 125–146 (Ph).

Bis(*N*-(dimethylamino)acetimidato-*N,O*)dichlorosilicon(IV) (4a). A mixture of 1.74 g (0.01 mole) of **6a**, 0.9 g (0.0052 mol) of tetrachlorosilane (**10**), and 20 mL of dry CH_2Cl_2 was stirred for 2 h at 20 °C under vacuum. The solvent was removed under reduced pressure. Recrystallization from 50 mL of hexane gave 1.2 g of **4a**, 80% yield, as colorless crystals with mp 135–140 °C: ^1H NMR ($CDCl_3$) δ 1.85

(34) (a) Kalinin, A. V.; Apasov, E. T.; Bugaeva, S. V.; Ioffe, S. L.; Tartakovskii, B. A. *Bull. Akad. Nauk SSSR* **1983**, 1413; *Chem. Abstr.* **1983**, *99*, 175871f. (b) Kalikhman, I. D.; Bannikova, O. B.; Volkova, L. I.; Gostevskii, B. A.; Yushmanova, T. I.; Lopirev, V. A.; Voronkov, M. G. *Bull. Akad. Nauk SSSR* **1988**, 460; *Chem. Abstr.* **1989**, *110*, 75608c. (c) Kalikhman, I. D.; Medvedeva, E. N.; Bannikova, O. B.; Fabina, N. G.; Larin, M. F.; Lopirev, V. A.; Voronkov, M. G. *Zh. Obshch. Khim.* **1984**, *54*, 477; *Chem. Abstr.* **1981**, *101*, 55158s.

(s, 6H, CMe), 2.95 (s, 6H, NMe_2), 3.13 (s, 6H, NMe_2); ^{13}C NMR ($CDCl_3$) δ 17.0 (CMe), 51.5, 52.3 (NMe_2), 166.5 (C=N); HRMS for M^+ ($C_8H_{18}Cl_2N_4O_2Si$), calcd 300.0576, found 300.0595.

Compounds **4b** and **4c** were prepared by the same method as **4a**.

Bis(*N*-(dimethylamino)benzimidato-*N,O*)dichlorosilicon(IV) (4b). Recrystallization from hexane afforded colorless crystals of **4b** in 72% yield: mp 167−170 °C; ^1H NMR ($CDCl_3$) δ 3.10 (s, 6H, NMe_2), 3.27 (s, 6H, NMe_2), 7.4−7.9 (m, 10H, Ph); ^{13}C NMR ($CDCl_3$) δ 52.2, 52.9 (NMe_2), 163.6 (C=N), 127−148 (Ph). Anal. Calcd for $C_{18}H_{22}Cl_2N_4O_2Si$: C, 50.82; H, 5.21; Cl, 16.67; N, 13.17; Si, 6.60. Found: C, 50.90; H, 5.30; Cl, 18.98; N, 13.08; Si, 6.72.

Bis(*N*-(dimethylamino)trifluoroacetimidato-*N,O*)dichlorosilicon-(IV) (4c). Colorless crystals with mp 116−117 °C were obtained directly from the reaction mixture in quantitative yield: ^1H NMR ($CDCl_3$) δ 3.26 (s, 6H, NMe_2), 3.33 (s, 6H, NMe_2); ^{13}C NMR ($CDCl_3$) δ 51.8, 52.1 (NMe_2), 156.1 (q, ^3J(C−F) = 39 Hz, C=N), 117.0 (q, ^1J(C−F) = 277 Hz, CF_3). Anal. Calcd for $C_8H_{12}Cl_2F_6N_4O_2Si$: C, 23.48; H, 2.96; Cl, 17.33; F, 27.86; N, 13.69; Si, 6.86. Found: C, 24.34; H, 3.44; Cl, 18.29; F, 26.68; N, 13.97; Si, 6.72.

Bis(*N*-(dimethylamino)benzimidato-*N,O*)(fluoro)phenylsilicon (18): ^1H NMR ($CDCl_3$) δ 2.25 (s, NMe_2, 3H), 2.63 (s, NMe_2, 3H), 2.70 (s, NMe_2, 3H), 3.21 (s, NMe_2, 3H), 7.96 (d, ^3J(H−H) = 8 Hz, *ortho* H, 1H), 8.09 (d, ^3J(H−H) = 8 Hz, *ortho* H, 1H), 6.6−7.8 (m, Ph, 13H); ^{13}C NMR ($CDCl_3$) δ 53.0, 50.7, 50.1 (NMe_2), 164.9, 164.8 (C=N), 145.6 (d, ^2J(C−F) = 43.6 Hz, *ipso* C(PhSi)), 138.0 (d, ^3J(C−F) = 8.7 Hz, *ortho* C (PhSi)), 136.7 (d, ^3J(C−F) = 7.3 Hz, *ortho* C (PhSi)), 127−147 (Ph); ^{29}Si NMR ($CDCl_3$) δ 148.6 (d, ^1J(Si−F) = 272.9 Hz).

Acknowledgment. We thank the Israeli Ministry of Absorption and Ministry of Sciences and Arts and the Israel Science Foundation (administered by the Israel Academy of Sciences and Humanities) for financial support. We thank Professor V. A. Pestunovich for helpful discussions and Dr. B. A. Gostevskii for assistance in handling the complexes.

JA9520474